Assemblies of Microfluidic Channels and Micropillars Facilitate Sensitive and Compliant Tactile Sensing

Bin Li, *Student Member, IEEE,* Ye Shi, *Student Member, IEEE,* Hui Hu, Adam Fontecchio, *Senior Member, IEEE* and Yon Visell, *Member, IEEE*

***Abstract*—Recent advances in soft electronics are enabling new devices that can stretch and conform to curved, soft, or dynamic surfaces, whether in engineering systems or the human body. However, the close coupling of mechanical and electronic behavior in these devices can limit performance and introduce artifacts. In order to mitigate negative effects, and to facilitate greater control over mechanical and electronic performance, we present a method for designing soft tactile sensors based on multi-layer heterogeneous 3D structures that combine active layers, containing embedded liquid metal electrodes, with passive and mechanically tunable layers, containing air cavities and micropillar array geometric supports. The assembled devices consist of thin membranes that integrate arrays of tactile sensors with 2 mm spatial resolution. They are produced using a soft lithography fabrication method based on the casting, alignment, and fusion of multiple functional layers in a soft polymer substrate. We have optimized the electronic and mechanical performance of these devices using numerical simulations. The results accurately predicted measured performance, making it possible to tailor both electronic and mechanical properties. These methods enable the design of tactile sensing arrays that are highly conformable and robust, and that possess a number of desirable attributes, including high sensitivity, monotonic output, good linearity, low cross-talk, low rate dependence, and low hysteresis. This may enable new applications in wearable electronics, healthcare, and robotics.**

***Index Terms*—Tactile Sensing, Soft Lithography, Wearability, Capacitance, Multi-layer**

I. Introduction

An encouraging trend in recent years has been the creation of electronic devices, including multimodal sensors, that can stretch to conform to arbitrary curved, soft, or dynamic surfaces, including the human body. The unique mechanical properties of these devices is creating new applications in areas ranging from wearable health monitors to electronic skin for robots. With these opportunities come new difficulties, due to the strong coupling of electronic and mechanical effects that these devices frequently entail. However, through careful design and materials selection, these challenges can be overcome, allowing these couplings can be utilized to improve device performance, as we demonstrate in the work presented here.

Stretchable tactile sensors could one day augment human and machine interactions with real-world environments, by mechanically tailoring interactions, and electronically capturing activities, in ways that evoke the remarkable functional characteristics of human skin. This could benefit applications in robotics, virtual reality, and prosthetics.

During touch interaction with real-world objects, contact surfaces are generally non-planar, and are instead typically curved and compliant, and may furthermore change dynamically according to the shape of the hand or the geometry of contact. Consequently, it is widely recognized that any electronic tactile sensing device that is to operate in unconstrained environments should be compliant, and adaptable to the surfaces involved. Most tactile sensors that have been developed utilize stiff substrates that are not able to significantly deform without failure. Even those devices that are able to flex (due to the use of flexible electronic substrates) can impair tactile sensing, since they largely impede the capture of shear strains, and make it difficult to maintain slip-free contact during shear interactions with a contact surface, as are commonly observed in touch, grasping, object lifting, and manipulation.

Recently, several researchers have proposed strategies for realizing tactile sensing devices that are constructed from stretchable materials [1–7], flexible substrates [8–11], or with geometries that admit deformation through fine articulation or meshing [12–15]. Among these, methods involving the embedding liquid metal alloy within soft synthetic polymers [1, 2, 6] or somewhat stiffer polydimethylsiloxane (PDMS) [16, 17], have received the greatest interest. The intrinsic stretchability of these materials makes them suitable for realizing soft electronic devices, including wearable electronics, that are able to conform to a wide range of surfaces and materials.

Although several approaches to the design and fabrication of compliant sensor arrays have been reported in the literature, current methods are not able to ensure that a device can function within a specified operating range of forces, or, more generally, meet application-dependent electronic or mechanical performance requirements. Rather, mechanical considerations of softness often constrain electronic performance. For example, we recently demonstrated that the sensitivity and effective operating range of soft, solid cast capacitive sensors is theoretically and empirically limited due to the existence of a non-monotonic regime at low strains [6, 7]. This cannot

Yon Visell and Hui Hu are with the Department of Electrical and Computer Engineering, Media Arts and Technology Program, and California NanoSystems Institute, University of Califonia, Santa Barbara, California 93106, USA e-mail: yonvisell@ece.ucsb.edu

Bin Li, Ye Shi and Adam Fontecchio are with the Department of Electrical and Computer Engineering, Drexel University, Philadelphia, PA, 19104 USA. e-mail: bin.li@drexel.edu

Manuscript received Jun 14, 2016.

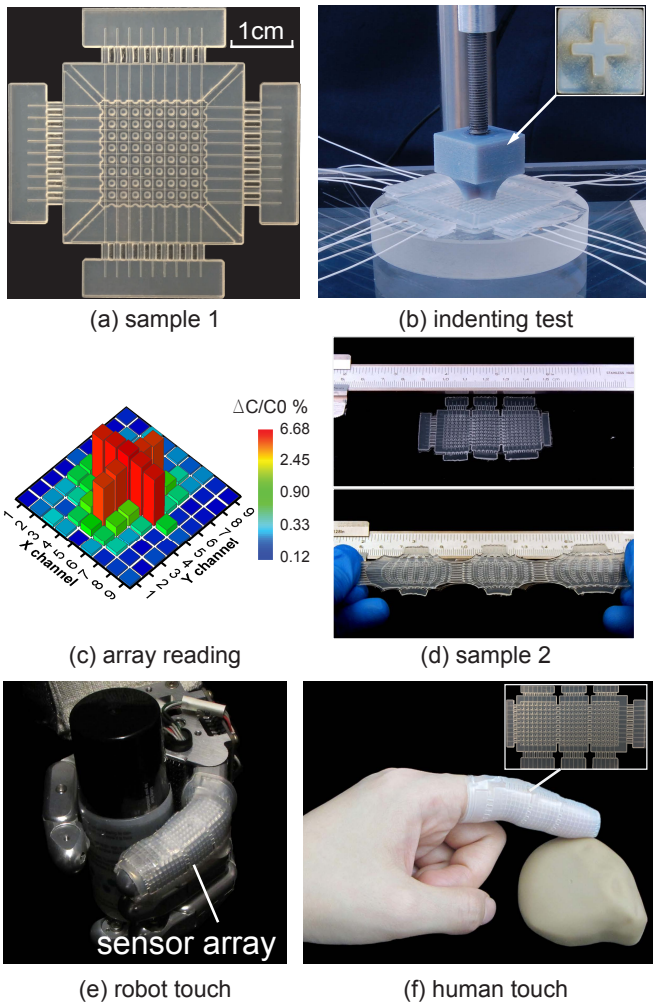

Fig. 1: Overview of the compliant tactile sensing arrays. a) The 9 × 9 tested sensor array. b) Indentation test on a flat surface. c) Measurements under indentation testing (300 μm depth). d) Stretching a 9 × 17 sensor. e,f) The compliance of the sensor allows it to be worn on a robot or human finger.

be trivially avoided (for example, by altering the material or geometry), due to the dependence of electronic measurements on volumetric strain. Several other undesirable effects can arise for similar reasons. These include mechanically-induced cross-talk, strain-rate dependence, hysteresis, and strain-induced channel collapse and electrical failure.

In order to mitigate such effects, and to facilitate greater control over mechanical and electronic performance, we have developed a design method for soft micromechanical devices, described here for the first time, based on a multi-layer heterogeneous 3D structure. It combines membranes with embedded soft electrodes, similar to those used in previous devices, with passive and mechanically tunable layers that contain air cavities. These cavities are separated by micropillar array geometric supports. After assembly, the resulting devices consist of thin membranes integrating arrays of tactile sensors. They are able to perform sensing while preserving high stretchability (over 200%, Fig. 1), spatial resolution, sensitivity, and dynamic response. In order to fabricate these devices, we have developed a soft lithography fabrication method based on the casting, alignment, and fusion of multiple functional layers in a soft, addition-cured polymer substrate. The method that we propose is simple, and yields three-dimensional geometric detail that would be more difficult to realize using other methods.

The present manuscript describes the design of tactile sensors that utilize this approach, and presents soft lithography methods for fabricating them. In order to better explain and analyze the mechanical and electronic performance of these devices, we performed numerical simulations. We used the results of simulations to optimize prototype sensors with 2 mm × 2 mm spatial resolution, which we then fabricated and tested under distributed (2D) loading conditions. Measurements were in close agreement with numerical predictions, and revealed that these devices were able to achieve high sensitivity, linear response, low cross-talk, and low levels of hysteresis. A graphical overview of the results is given in Figure 1. The following sections of the paper review our approach to modeling these devices, the use of numerical simulations to guide their design, and a multi-layer soft lithography fabrication method used to produce them. We also present the results of single-point testing and tactile imaging with sensors fabricated using these methods.

In summary, the main contributions of this paper are a new design for soft micromechanical sensors for capacitive imaging, a demonstration that this design is able to overcome fundamental limitations on the sensitivity of solid cast capacitive sensors, a method for efficient fabrication of heterogeneous, multi-layer soft tactile sensors, and a demonstration that the resulting sensors are able to perform tactile imaging on flat and curved surfaces with high performance, including high spatial resolution, dynamic range, sensitivity, and low crosstalk.

II. Multilayer Sensor Design

In order to realize resilient, mechanically tunable, and electronically responsive tactile sensors, we combine methods for designing capacitive array sensors with soft lithography techniques for creating intrinsically deformable, heterogeneous membranes.

A. Operating principle

Mutual capacitance sensing is based on the change in capacitance between two electrodes that accompanies changes their geometric configuration or the proximity of dielectric materials in their vicinity. When pressure is applied to a compliant capacitance sensor, the distance between the electrodes is reduced, yielding an increase capacitance, assuming that other factors, such as the electrode geometry, are unchanged. Tactile sensing arrays based on mutual capacitance are often formed, as in our device, through the arrangement of parallel electrodes in orthogonal directions on two layers. We refer to the region of closest approach between each pair, consisting of an upper and lower electrode, as a sensing cell. In our device, the electrodes are embedded in a highly elastic substrate, so that a surface pressure applied to the device will elicit

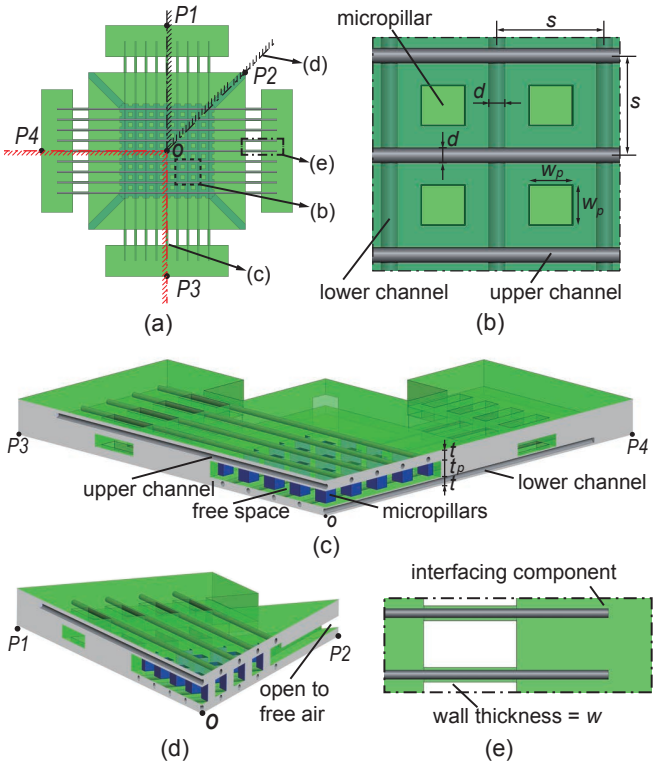

Fig. 2: Structure of the multilayer stretchable tactile sensing array. a) The overview of a 9×9 sensing array. b) Magnified top-view, showing the configuration of microchannels and micropillars. c-e) Section views of the sensing array, showing the sensor's multilayer structure.

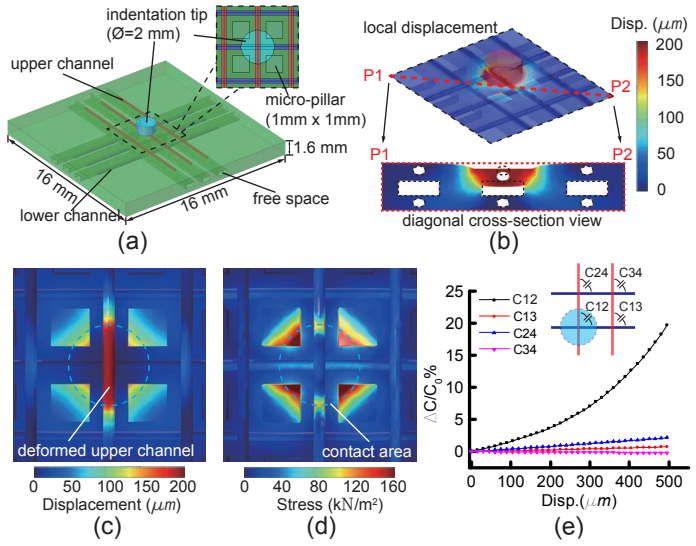

Fig. 3: Finite element model and simulation results. a) Structure of the simulated model, using the same parameters of the sample shown in Figure 2. b) Cross-section view of displacement along a 45° diagonal section. c, d) Top-view of the displacement and stress, respectively, of the sensing cell under compression and its surrounding micropillars. e) Capacitance change (%) with normal indentation (μm).

a strain that reduces the inter-electrode distance, increasing mutual capacitance between them. By measuring this change in mutual capacitance, and combining this with electronic and mechanical measurements performed during device calibration, we are able to map the sensed capacitance values to the local strain or pressure, realizing an electronic sensor.

B. Sensor design

Our design method yields multilayer sensing arrays in the form of a composite membrane constructed from three layers. Two of these layers contain arrays of soft electrodes, and a third layer contains an array of micropillar structures (Fig. 2). To achieve high levels of compliance, we cast these layers from low modulus synthetic polymer, and combine them to yield a thin multi-layer membrane (thickness t).

We design the electrode layers as soft rectangular plates containing parallel arrays of microfluidic channels. The channels (diameter d), initially empty, are embedded in the elastic substrate, and subsequently filled with electrically conductive liquid metal alloy (eutectic Gallium Indium, eGaIn). The microchannel spacing is constant within each layer, and their center-to-center spacing, s, determines the spatial sensing resolution.

In order to make it possible to tune the operating range of pressures according to application requirements, we introduce

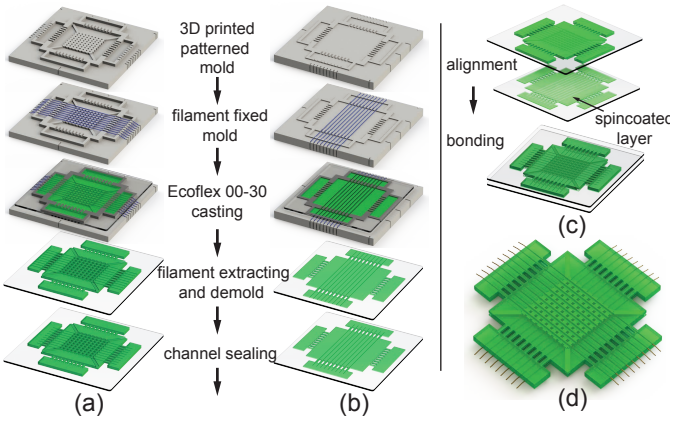

Fig. 4: Overview of the procedure to fabricate the proposed stretchable sensing array. a, b) Preparation of the upper part and the lower part. c) Align and bond the two parts together. d) Functionalize the sensing array by filling channels with eGaIn, and inserting electrodes to form the electronic interface.

a third, intermediate, layer (thickness t_p) comprising a two-dimensional array of N_p small, square micropillars (width w_p). The micropillars are centered between the microchannels, when viewed from above and are separated by a contiguous free space. By reducing the pillar width w_p, the effective stiffness of the layer is reduced, and the pressure-induced strain increased, yielding a more rapid increase in capacitance with pressure. By way of illustration, for small strains, the layer can be modeled as a linear elastic solid, with elastic modulus E. In this regime, the effective stiffness K of the micropillar layer, with cross-sectional area $A = N_p w_p^2$, is

approximately

$$K = EA/t_p = EN_p w_p^2/t_p \ . \quad (1)$$

More generally, for a nonlinear material with constitutive behavior $\sigma(\epsilon)$ describing the change in stress $\sigma = F/A$ with strain $\epsilon = x/t_p$, where A is the area, the force F and displacement x in uniaxial loading are related by a surface integral over the ensemble of N_p pillars

$$F(x) = \sum_{i=1}^{N_p} \int_{A_p} dz \ \sigma_z(\epsilon) = N_p w_p^2 \ \overline{\sigma}(\epsilon), \quad \epsilon = x/t_p \quad (2)$$

where $\overline{\sigma}$ is the average surface pressure, and $A_p = w_p^2$ is the surface area of a pillar. We note that our design does not depend explicitly on this model. However, Equations (1) or (2) illustrate the role of the square of feature width w_p^2 in determining the force that results from a given displacement x, and the role of thickness t_p in scaling the operating displacement. In earlier work [6], we demonstrated that solid mechanics, when combined with a transmission line model of mutual capacitance, is sufficient to accurately predict the sensor output, indicating that the aforementioned parameters are suitable for tailoring sensor performance.

To facilitate robust data acquisition, we further introduce four interface components, consisting of arrays of short segments of channels that are independently cast and connected to the main sensing membrane with thin-wall microchannels (Figure 2(a,e)). These offset structures isolate the microchannels from mechanical stresses induced during testing, an important consideration during prototyping.

We designed a prototype device with upper and lower layers of microchannels (diameter $d = 300$ μm, spacing $s = 2$ mm), embedded in upper and lower polymer layers ($t = 500$ μm); see Figure 1 (a). The micropillar layer has thickness $t_p = 600$ μm and an 8×8 array ($N_p = 64$) of pillars with width $w_p = 1$ mm.

III. Modeling and Numerical Simulation

To validate the sensor design, we performed numerical simulations using multiphysics finite element analysis (FEA), including electrostatic, fluid, and solid mechanics effects. We used the simulation to investigate aspects of sensor performance, including sensitivity, linearity, and robustness. We designed a CAD model and introduced it into a numerical simulation (COMSOL Multiphysics, Comsol Inc.) with structure parameters that mirror those of our prototype design. For computing efficiency, this model included only three upper and three lower channels in the model, realizing nine sensing cells. The modeled device was otherwise identical to the prototype design described in Section II, with a thickness of 1.6 mm.

We simulated the device response (Fig. 3) under indentation by a disc of diameter 2 mm that was placed concentrically above a sensing cell at the center of the array. The sensor was supported by a rigid platform and tested under simulated displacement-controlled loading up to 200 μm. From the simulation, we obtained strain and stress distributions, and capacitances for the 9 sensing cells (Fig. 3). To validate the design approach, we further analyzed the deformation of the microchannels, and the coupling between pressed and unpressed sensing cells (Fig. 3(b,c,d)).

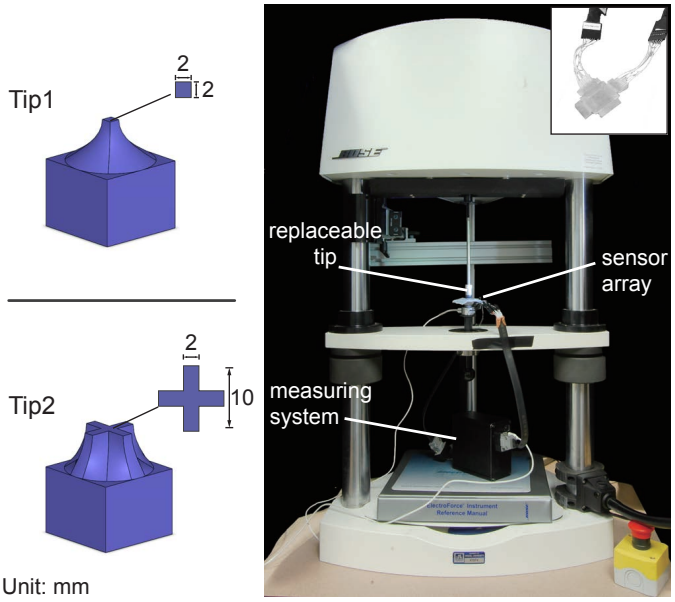

Fig. 5: Indenting tips used for characterization and the programmable mechanical testing system used in the experiments. The inset figure shows the connection between the sensor and data acquisition electronics.

From the simulation results, compression reduced the distance between the upper and lower channel, yielding greater mutual capacitance (Figure 3(b,c)). There was substantial vertical compression of the upper channel and the four surrounding micropillars. The eight unpressed sensing cells showed little displacement (less than 1%), indicating that mechanical coupling between the channels was minimized, as intended, by our design. Under indentation, the small magnitude of stress at the compressed upper channel indicates that the channel geometry, and electrode integrity, remained intact under compressive loading (Figure 3(d)).

Due to the decrease in distance between upper and lower channels, the capacitance increased monotonically with compressive strain (Figure 3(e)). Capacitance increased at very small displacements, reflecting the high sensitivity of the device. The capacitance of neighboring sensing cells remained nearly unaffected, indicating a high level of electronic decoupling that is achieved in this design.

IV. Multilayer Soft-Lithography Fabrication

In order to fabricate the devices that we designed and simulated, we developed a new multilayer fabrication technique, building on existing soft lithography methods. The approach integrates a 3D printing based casting technique that we recently developed (we refer to it as *direct filament casting*), and that facilitates the fabrication of networks of liquid metal electrodes in very low modulus polymer membranes [7]. The process involves the creation of separate functional components that are aligned, bonded (Fig. 4), and finally

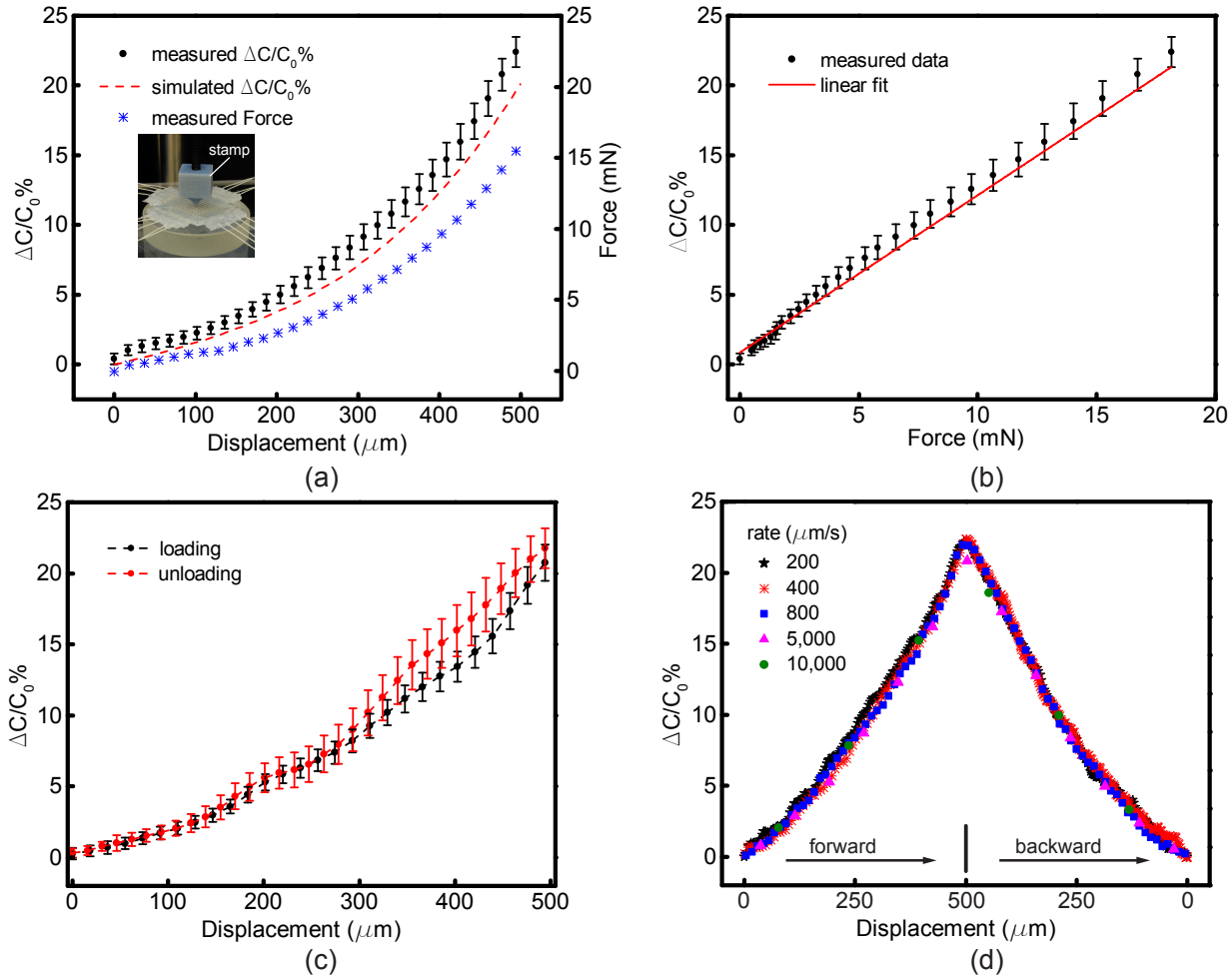

Fig. 6: Characterization of sensing cell performance under strain controlled loading. a) Change in capacitance (black dot, %) vs. strain (μm), showing good agreement with simulations (red dashed line). Error bars: 1 standard deviation. Measured force (μN) is shown in blue. Inset: Test configuration. b) Capacitance changed with force in a linear fashion up to 20 μN. c) Hysteresis of forward and backward indenting cycle. d) Sensor response to strain applied at different rates (200 μm/s to 10,000 μm/s), demonstrating remarkably little strain-rate dependence.

functionalized through the introduction of liquid metal into conductive microchannels.

The preparation of the upper and lower components each proceeds with the creation of 3D CAD models of negative molds and a fixture frame that are used for casting (Figure 4(a, b)). These are printed using a photopolymer 3D printer (Object30, Stratasys Ltd.). The upper component contains the negative mold of the micropillar array. The mold surface is cleaned with isopropyl alcohol and dried, and a single monofilament (South Bend Monofilament, 200 or 300 μm diameter) spray-coated with surface release agent (Ease Release 200, Smooth-On, Inc.) is wound around the mold, following a path determined by fixture teeth in the mold. The bulk substrate of the device consists of an addition cured polymer elastomer (Ecoflex 00-30, Smooth-On, Inc.). This material is compliant and stretchable with M100 modulus of 10 psi, 900% elongation at break, 0.1% shrinkage and dielectric strength of 13.8×10^6 V/m. Depending on application requirements, other soft polymers could be used.

Additive liquid synthetic polymer components (Ecoflex 00-30, as noted) are mixed, degassed and poured into the mold. A flat acrylic cover is used to close the mold, squeezing out extra polymer material. After curing for 6 hours, the filament is extracted from the mold. The cast mold is heated to 60 °C for 15 minutes, to facilitate demolding. The channels are sealed via syringe injection of liquid polymer, using a custom bracket and aligner. A bonding film of liquid polymer (thickness 100 μm) is spin-coated on the lower component (Fig. 4(c)), and the upper and lower components are aligned, centering each micropillar between microchannel intersections in the array. After partial curing (30 minutes), the parts are bonded and cured for six hours. The sensing array is then functionalized by filling all channels with liquid metal alloy (eGaIn, 75% Ga, 25% In by mass, melting point 15.7 °C [18, 19]) under syringe injection. Since the introduction of bubbles into the channel would impair performance, eGaIn is carefully introduced under syringe injection, while maintaining a seal around the injection point. They are terminated by inserting

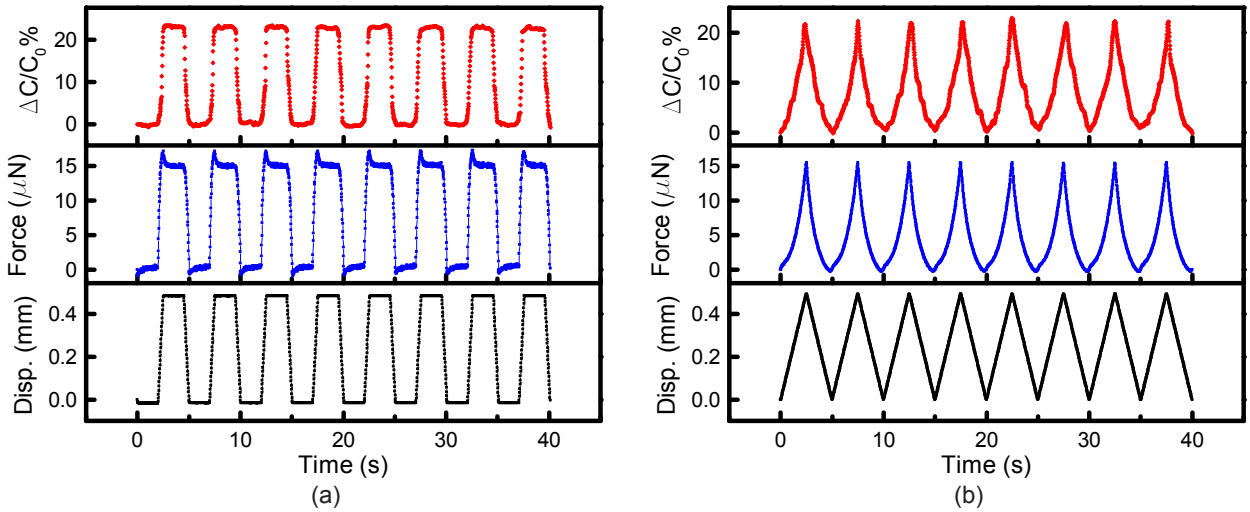

Fig. 7: A single sensing cell was tested with two different strain-controlled load functions: a) Trapezoidal load function with transient strain rate of 1000 μm/s , and b) Ramp load function with strain rate of 200 μm/s. The data shown were all captured in succession in real time, without further processing or averaging. Measurement uncertainty: See Fig. 6a.

wires and further sealing. Using this method, it is possible to control the geometry and position of microchannels with an accuracy of approximately 10 μm [7].

The resulting device, consisting of a 9 $\times$ 9 array in one prototype, Figure 1(a), remains soft and highly compliant. We have employed the same method to fabricate sensors that varied in geometry and structural design, and hence stiffness, including a 9 $\times$ 17 device with rectangular shape, suitable for use in robotic or wearable sensing (Fig. 1(d-f)). Similar to the solid cast devices described in our prior work [7], due to the very low elastic modulus of the substrate, the resulting devices recoverably deform to applied strains greater than 200% strain without mechanical or electronic damage. By selecting a different commercially available polymer in the same family, one can realize devices that are softer or stiffer, according to application requirements.

V. Characterization and Functional Testing

We characterized the mechanical and electronic performance of the device under servo controlled indentation using stamps of variable geometry and flat or curved support surfaces. To facilitate this, we designed custom electronics for matrix-addressed capacitance sensing, using a dedicated integrated circuit (AD7746, Analog Devices) and microcontroller. This yielded a sensing system with excellent sensitivity (measured to be approx. 10 femtofarad, fF) and resolution (approximately one attofarad, 10^{-18} F).

We tested the performance of a 9$\times$9 sensor array in three configurations. Two of these assessed the sensitivity and dynamic range of individual sensing cells in the array, and one assessed the utility of the device for two-dimensional tactile imaging. In the single cell tests, the quasi-static and dynamic response were characterized during indentation testing with a circular stamp of diameter of 2 mm. Displacement-controlled loading was performed via a programmable mechanical test system (Figure 5, ElectroForce 3200 Series III, Bose Corp.). We concurrently recorded capacitance using the electronics described above. Dynamic loads with a step function profile, and with ramp function profiles (load rates 200 μm/s to 10,000 μm/s) were used to assess the time-varying response (Fig. 6). We recorded the dynamic response during loading and unloading in order to investigate hysteresis effects.

During the multi-cell tests, the use of the sensing array for tactile imaging was investigated by indenting the array with a cross-shaped stamp (width 10 mm, edge width 2 mm). The array was indented up to values reaching 300 μm. In a further test, we assessed the device performance with the sensor supported on a curved acrylic surface, during indentation with the cross-shaped stamp to depths as high as 300 μm. In each experimental condition, averages of 10 measurements were recorded for analysis.

VI. Results and Discussion

The quasi-static response of the device is well captured via the change in capacitance with force and displacement during strain-controlled loading (Figure 6). The measured results show excellent qualitative and quantitative agreement with finite element simulations (Figure 6a). Under zero load, the capacitance was 63.3 fF (i.e., 6.33×10^{-14} farad, standard deviation 5.8×10^{-16} F). Under displacement-controlled loading (Figure 6), measured and simulated capacitance rose monotonically by 25% under an imposed strain that increased by 30%, a region that spans 42 dB of dynamic range. The change in capacitance with applied strain was mildly nonlinear, while a nearly linear variation in capacitance was observed as a function of force. This is consistent with the high-strain regime that we observed with simpler, solid cast devices [6]. However, at low strains, the utility of the latter devices was greatly limited by non-monotonic behavior. In contrast, the monotonic performance that we observed with the device tested here validates the multi-layer design approach presented here.

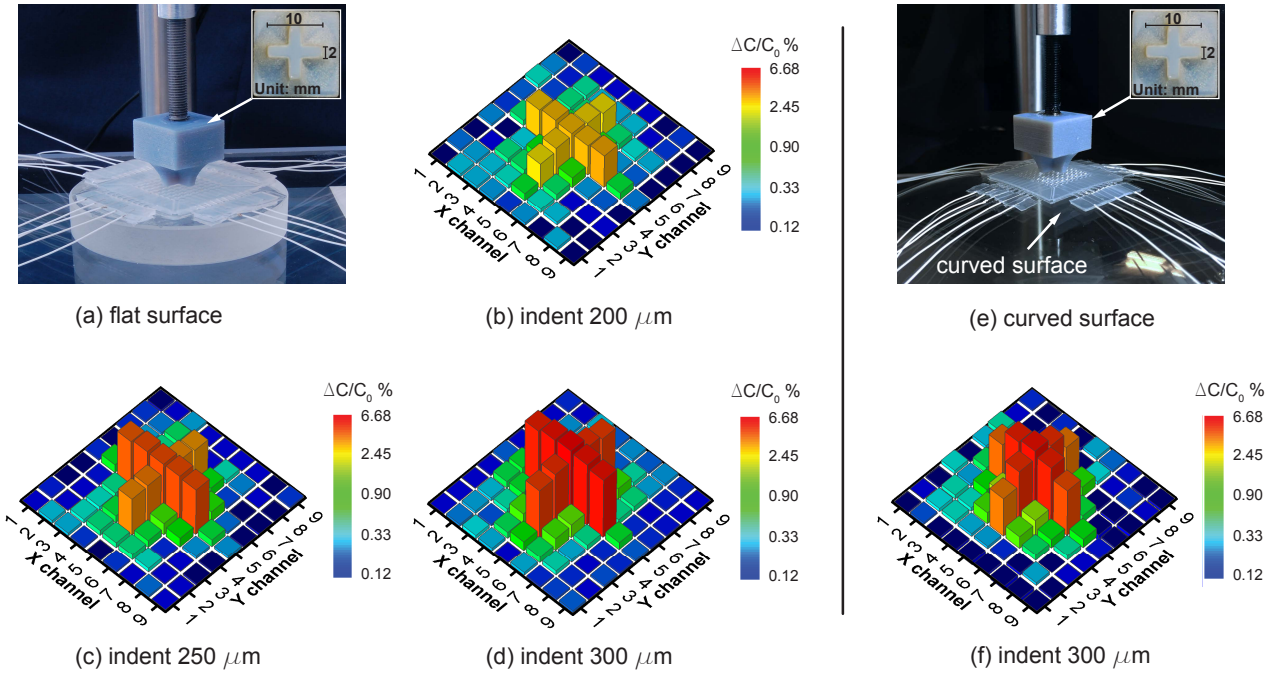

(a) flat surface (b) indent 200 μm (e) curved surface

(c) indent 250 μm (d) indent 300 μm (f) indent 300 μm

Fig. 8: Tactile imaging (average of 10 measurements) with a 9×9 sensing array, using a cross-shaped indentation stamp. a) The sensing array was indented upon a flat surface. b-d) The measured change of capacitance in each cell of the sensing array under an indentation of 200 μm, 250 μm, and 300 μm reaches as high as 7%, with standard deviation 0.3%. e,f) Tactile imaging as the sensing array conformed to a curved surface yields measurements that are highest at the center of the stamp, near its closest approach to the curved surface (radius of curvature 15.5 cm; measurement standard deviation 0.3%)

.

In analyzing the dynamic response of the sensor, we found minimal levels of hysteresis, which was typically only observable at the highest strain levels, 300 μm to 500 μm (Figure 6 (c)). Indeed, there was almost no variation in sensor output with loading rates from 200 μm/s to 10,000 μm/s (Figure 6). The sensor output closely followed the indentation profile in both trapezoidal and ramp loading conditions (Figure 7). During trapezoidal (quasi-step) loading, capacitance closely tracked displacement despite significant overshoot in force measurements (which are the normal result of rapid loading of a soft polymer).

In a last set of experiments, we investigated the ability of the sensor array to perform tactile sensing of distributed loads while conforming to flat or curved surfaces. Output from the sensor array precisely mirrored the shape of the indentation stamp, and varied only in magnitude with indentation depth (Figure 8). Cross-talk to adjacent (unpressed) sensing cells was minimal, less than 1% ([7]). This was the case in spite of the intrinsic solid mechanical coupling of adjacent sensing cells in the array, which was minimized due to the thinness of the device. Similar tactile imaging performance was observed when the sensor was supported on a curved surface, with the sensor output changing solely due to the nearer approach of points at the apex of the support surface, which was near the center of the stamp. A greater strain is produced at the center of the stamp, which is closest to the support surface, due to the curvature of the latter. As expected from our point measurements (Fig. 6), this increased strain is reflected in an augmentation (on the order of 3%) of the capacitance at the stamp center, which is not a measurement artifact, but a veridical reflection of the difference in loading across the sensor.

VII. Conclusion

In this paper, we describe soft micromechanical sensors for capacitive tactile imaging. The sensors use arrays of compliant electrodes embedded in multi-layer soft polymer membranes. The functional properties of these devices are facilitated by via microfluidic channels and micropillars, which allow for capacitance sensing and mechanical tuning. We presented principles guiding the design of these devices and describe soft lithography methods for fabricating them. These methods have proven robust, repeatable, and amenable to fabricating more complex geometries than can be easily realized with photolithography methods. We performed three dimensional multiphysics (mechanical and electrical, coupled) finite element simulations in order to explain, analyze the mechanical and electronic performance, and used the results to optimize the design of prototype sensors (9×9 sensing cells, 2×2 mm spatial resolution), which we subsequently fabricated and tested under distributed (2D) and time-varying loading conditions.

The observed performance was in close agreement with numerical predictions. Through them, we determined that these devices could achieve high sensitivity, monotonic output, a remarkably linear force-capacitance relationship, excellent

tactile imaging, low crosstalk, low load-rate dependence, and low levels of hysteresis. The devices performed similarly whether conforming to flat or curved surfaces.

The resulting tactile sensors are robust, highly conformable, and may be suited to emerging applications in biomedical imaging of soft tissues during clinical palpation, to wearable sensing for human-computer interaction, or as electronic skin for robotic manipulators or prosthetic limbs, where it may facilitate interaction (grasping and manipulation) via touch. Through the selection of (polymer) materials and geometric parameters, the device can readily be adapted to meet application requirements, including compliance, sensitivity, resolution, and dynamic range.

Despite the promising nature of these results, there are several areas for future improvement. The use of gallium indium liquid metal alloy electrodes limits the operating range of temperatures to those greater than the melting point of the conductor (15.7 °C for the alloy used in our device). However, gallium indium alloys with higher melting point are commercially available and, moreover, low melting point ionic conductors could also be used, since the current carrying requirements for capacitance sensing are low. Other areas of potential improvement include refining the fabrication techniques to enable further miniaturization, the improving the mechanical and electronic design of the interconnect-sensor junctions, the introduction of further conducting and insulating layers to further improve electronic performance, and selecting polymers with higher dielectric constants to increase the operating range of capacitance.

ACKNOWLEDGMENTS

This work was supported by NSF awards No. 1446752 and 1527709.

REFERENCES

[1] Y.-L. Park, C. Majidi, R. Kramer, P. Brard, and R. J. Wood, "Hyperelastic pressure sensing with a liquid-embedded elastomer," *Journal of Micromechanics and Microengineering*, vol. 20, no. 12, p. 125029, 2010.

[2] P. Yong-Lae, C. Bor-Rong, and R. J. Wood, "Design and fabrication of soft artificial skin using embedded microchannels and liquid conductors," *Sensors Journal, IEEE*, vol. 12, no. 8, pp. 2711–2718, 2012.

[3] P. J. Codd, A. Veaceslav, A. H. Gosline, and P. E. Dupont, "Novel pressure-sensing skin for detecting impending tissue damage during neuroendoscopy," *J Neurosurg Pediatr*, vol. 13, no. 1, pp. 114–21, 2014.

[4] J. B. Chossat, P. Yong-Lae, R. J. Wood, and V. Duchaine, "A soft strain sensor based on ionic and metal liquids," *Sensors Journal, IEEE*, vol. 13, no. 9, pp. 3405–3414, 2013.

[5] A. Fassler and C. Majidi, "Soft-matter capacitors and inductors for hyperelastic strain sensing and stretchable electronics," *Smart Materials and Structures*, vol. 22, no. 5, p. 055023, 2013.

[6] B. Li, A. K. Fontecchio, and Y. Visell, "Mutual capacitance of liquid conductors in deformable tactile sensing arrays," *Applied Physics Letters*, vol. 108, no. 1, p. 013502, 2016.

[7] B. Li, Y. Gao, A. Fontecchio, and Y. Visell, "Soft capacitive tactile sensing arrays fabricated via direct filament casting," *Smart Materials and Structures*, vol. 25, no. 7, p. 075009, 2016.

[8] D. J. Lipomi, M. Vosgueritchian, B. C. Tee, S. L. Hellstrom, J. A. Lee, C. H. Fox, and Z. Bao, "Skin-like pressure and strain sensors based on transparent elastic films of carbon nanotubes," *Nat Nanotechnol*, vol. 6, no. 12, pp. 788–92, 2011.

[9] W. Hu, X. Niu, R. Zhao, and Q. Pei, "Elastomeric transparent capacitive sensors based on an interpenetrating composite of silver nanowires and polyurethane," *Applied Physics Letters*, vol. 102, no. 8, p. 083303, 2013.

[10] Y. Yao, S.; Zhu, "Wearable multifunctional sensors using printed stretchable conductors made of silver nanowires," *Nanoscale*, vol. 6, no. 4, p. 2345, 2014.

[11] O. A. Araromi, S. Rosset, and H. R. Shea, "High-resolution, large-area fabrication of compliant electrodes via laser ablation for robust, stretchable dielectric elastomer actuators and sensors," *ACS Applied Materials & Interfaces*, vol. 7, no. 32, pp. 18 046–18 053, 2015, pMID: 26197865.

[12] D.-H. Kim, N. Lu, R. Ma, Y.-S. Kim, R.-H. Kim, S. Wang, J. Wu, S. M. Won, H. Tao, A. Islam, K. J. Yu, T.-i. Kim, R. Chowdhury, M. Ying, L. Xu, M. Li, H.-J. Chung, H. Keum, M. McCormick, P. Liu, Y.-W. Zhang, F. G. Omenetto, Y. Huang, T. Coleman, and J. A. Rogers, "Epidermal electronics," *Science*, vol. 333, no. 6044, pp. 838–843, 2011.

[13] N. L. J. A. R. Dae-Hyeong Kim, "Materials for multifunctional balloon catheters with capabilities in cardiac electrophysiological mapping and ablation therapy," *Nature Mater.*, vol. 10, no. 4, p. 316, 2011.

[14] J. W. Jeong, M. K. Kim, H. Cheng, W. H. Yeo, X. Huang, Y. Liu, Y. Zhang, Y. Huang, and J. A. Rogers, "Capacitive epidermal electronics for electrically safe, long-term electrophysiological measurements," *Adv Healthc Mater*, vol. 3, no. 5, pp. 642–8, 2014.

[15] Y. Ming, P. B. Andrew, L. Nanshu, S. Yewang, L. Rui, C. Huanyu, A. Abid, H. Yonggang, and A. R. John, "Silicon nanomembranes for fingertip electronics," *Nanotechnology*, vol. 23, no. 34, p. 344004, 2012.

[16] R. D. Ponce Wong, J. D. Posner, and V. J. Santos, "Flexible microfluidic normal force sensor skin for tactile feedback," *Sensors and Actuators A: Physical*, vol. 179, pp. 62–69, 2012.

[17] D. J. Cohen, D. Mitra, K. Peterson, and M. M. Maharbiz, "A highly elastic, capacitive strain gauge based on percolating nanotube networks," *Nano Lett*, vol. 12, no. 4, pp. 1821–5, 2012.

[18] S. J. French, D. J. Saunders, and G. W. Ingle, "The system gallium-indium," *The Journal of Physical Chemistry*, vol. 42, no. 2, pp. 265–274, 1937.

[19] M. D. Dickey, R. C. Chiechi, R. J. Larsen, E. A. Weiss, D. A. Weitz, and G. M. Whitesides, "Eutectic gallium-indium (egain): A liquid metal alloy for the formation of stable structures in microchannels at room temperature," *Advanced Functional Materials*, vol. 18, no. 7, pp. 1097–1104, 2008.

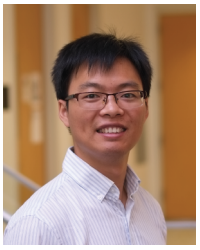

Bin Li received the B.S. and M.S. degrees in electronic science and technologies, and physical electronics from Xi'an JiaoTong University, Xi'an, China, in 2006 and 2009 respectively. He was electronics engineer from 2009 to 2012 in the Optical Network R&D department at Huawei Technologies in Shenzhen, China. Since 2012, he has worked in the Nanophotonics and RE Touch Laboratories at Drexel University, where he is a Ph.D. candidate in Electrical and Computer Engineering. His interests include novel wearable electronics and tactile sensing systems, with applications in haptics, medicine, prosthetics, and robotics.

Ye Shi received the B.Sc. degree in Automation from Harbin Institute of Technology, China in 2013, and M.S. degree in Electrical Engineering from Drexel University, Philadelphia, PA, USA, in 2016. He has been a student researcher at the RE Touch Lab and the Drexel Nanophotonics Lab since 2015. His interests include control, systems, machine learning, robotics and haptics. His current research includes system optimization, image processing, electronics design, data analysis and soft electronics.

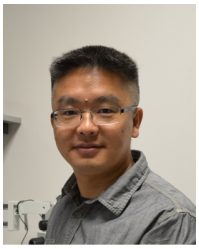

Hui Hu received the B.Eng. and M.Eng. degrees from Sun Yat-sen University, China in 2003. He has undertaken research and development in the field of embedded system development in industry and academia for more than a decade. He is currently a research scholar in the Department of Electronic and Computer Engineering at the University of California, Santa Barbara.

Adam Fontecchio is a Professor in the Department of Electrical and Computer Engineering at Drexel University and is Vice-Dean of the Graduate College. He is the inaugural Director of the Center for the Advancement of STEM Teaching and Learning Excellence (CASTLE), serves as Vice-Chair of the IEEE Philadelphia Section, and is a member of the IEEE-USA K-12 STEM Literacy Committee. His research focuses on the area of nanophotonics. He has served as PI or Co-PI on $>$ \$18M in sponsored research funding, and authored $>$90 peer-reviewed papers. He was selected as the 2015 Delaware Valley Engineer of the Year, and is the recipient of a NASA New Investigator Award, the Drexel Graduate Student Association Outstanding Mentor Award, the Drexel University ECE Outstanding Research Achievement Award and the International Liquid Crystal Society Multimedia Prize.

Yon Visell received the PhD Degree in Electrical and Computer Engineering from McGill University (2011), and MA and BA degrees in Physics (Univ. Texas-Austin, Wesleyan Univ.). Since 2015, he is Assistant Professor of Media Arts and Technology and Electrical and Computer Engineering at the University of California, Santa Barbara, where he directs the RE Touch Lab. Assistant Professor (2012-2015) in the ECE Department at Drexel University. Post-Doctoral Fellow (2011-2012) at the Inst. of Intelligent Systems and Robotics, Université Pierre et Marie Curie. He has been employed in industrial R&D for sonar, speech recognition, and music DSP at several high-technology companies. His research interests include whole-hand haptic function, haptic engineering, and soft robotics.